

Development of Various Semiconductor Quantum Devices

Tsukuru KATSUYAMA

Semiconductor quantum devices, composed of semiconductor quantum wells and superlattices, are widely used in our daily lives as key devices for opto-electronic equipment. The quantum well structure consists of alternating ultra-thin semiconductor films in which electrons and holes are confined. This structure gives rise to discrete energy levels and minibands in their potential wells, and thus induces new properties that cannot be obtained in a bulk material. These properties have enabled opto-electronics devices to have various new functions and high performance.

This paper describes various semiconductor quantum photonic devices developed in Sumitomo Electric for applications in a wide spectrum range of 1 to 10 μm . These devices include a semiconductor quantum well laser and modulator for high speed optical communication, quantum cascade laser for environmental gas analysis, and near-infrared imaging sensor for life science applications.

Keywords: quantum well, superlattice, semiconductor laser, quantum cascade laser, infrared sensor

1. Introduction

Semiconductor quantum well structure, including superlattice structure, is one of the greatest inventions in the field of compound semiconductor. The quantum well structure consists of alternating ultra-thin semiconductor films, in which electrons and holes are confined. Therefore, electrons and holes show two-dimensional behavior which induces new properties of material. This structure was proposed by Esaki and Tsu in 1969⁽¹⁾ and has become the basis of innovative technologies to produce high performance semiconductor devices.

In the early stage of development of quantum well technologies, the research of carrier transport in the quasi-two dimensional system had been performed and various devices were invented such as a high electron mobility transistor (HEMT)⁽³⁾ by applying modulation doping technology⁽²⁾ and a resonant tunneling transistor⁽⁴⁾ using wave function engineering. Meanwhile, the research in optical properties of quantum well structure led to the invention of various optical devices such as a quantum well laser⁽⁵⁾, a quantum dot laser⁽⁶⁾ an electro-absorption modulator, and a quantum cascade laser⁽⁷⁾.

We expect that this profound technology will continue to provide high performance and new functional semiconductor devices.

Sumitomo Electric Industries, Ltd. started the research and development of compound semiconductor materials in the 1960s and semiconductor devices in the middle of the 1980s in order to establish optical communication business integrating technology from materials, devices to systems. We have developed various kinds of high performance semiconductor devices by applying quantum well technology^{(8),(9)}.

This paper describes how this technology has been applied to various optical devices used in the field of information communication, life science, and environmental protection.

2. Quantum Well Structures and Materials

First, the origin of unique physical properties induced in quantum well structure is explained. **Figure 1** describes the energy state of quantum well structure. In the structure where two compound semiconductors with different band gaps pile up alternatively, electrons and holes are confined in the lower band gap layers. The thickness of the lower band gap layer approaches to the electron mean free path (several tens of nanometers), energy levels of the electron in the conduction band and the hole in the valence band are quantized. In the valence band, each hole energy level is split into two energy levels (heavy hole and light hole). This phenomenon is called quantum size effect. Then, the density of states in the conduction and valence band becomes a staircase which is very different from parabolic in bulk crystal as shown in **Fig. 1**. Therefore, the density of states near the minimum energy gap increases significantly. Reflecting this, the optical gain spectrum width becomes narrower and optical gain dramatically improves. Perform-

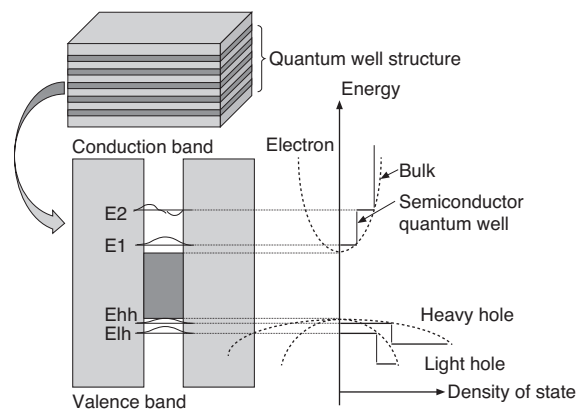


Fig. 1. Energy state of quantum well structure

ance improvement by introducing quantum well structure to semiconductor lasers is attributed to this phenomenon. In addition to the quantum size effect, several unique effects which cannot be obtained in the bulk material, such as electro-absorption effect and tunneling effect, have also been applied to develop high performance and new functional devices.

Table 1 summarizes the application areas of the device, the type of the device, the type of quantum well structure, and material combinations from a view point of wavelength that can be covered. Although application areas listed for each wavelength region are not limited to this wavelength region, the application fields of information and communications, life sciences, and environmental protection and security correspond to the wavelength region of low loss optical fiber, the absorption region of biological components, and the fundamental vibration of the molecule and the black body radiation at near room temperature, respectively.

The wavelength that can be covered by quantum well structure is determined by the combination, composition and thickness of material that form the quantum well structure. By controlling these parameters, the effective band gap or optical transition energy can be designed.

In this paper, we describe quantum well structures based on the material system that can be formed on InP substrate.

In the wavelength region used for optical fiber communication (1.2-1.7 μm), GaInAsP and AlGaInAs material systems are used to form type I quantum well structure in which smaller band gap material is sandwiched by larger band gap materials as shown in Tabel 1. In the type I structure, since electrons and holes are confined in the smaller band gap material, optical transition takes place between the quantized energy level formed in conduction and valence band with a high efficiency.

In the wavelength region from 1.7 μm to 3 μm , there is no material system that can form type I structure on the InP substrate. Therefore, the quantum well structure called type II using interband transition between the adjacent materials has been devised to form a smaller band gap. The effective band gap of InGaAs/GaAsSb material systems can

be decreased to about 3 μm . Since electrons and holes are spatially separated in type II structure, optical transition efficiency is lower than that of type I structure.

In the wavelength region longer than 3 μm , intersubband transition using large conduction band offset of AllnAs/InGaAs material systems can be applied.

Molecular Beam Epitaxy (MBE) and Organometallic Vapor Phase Epitaxy (OMVPE) have been used for the growth of these quantum well structures. MBE is a crystal growth method that is performed using physical adsorption by irradiating the molecular beam in an ultrahigh vacuum chamber. Since MBE is a high vacuum process, the crystal quality and growth process can be characterized and controlled by real time monitoring and can form very abrupt hetero-interface. On the other hand, OMVPE is the method of depositing semiconductor film by thermal decomposition of organometallic sources and suitable for the growth of phosphorus compounds and mass production. OMVPE is also suitable for selective area growth which is essential for realizing high performance devices and monolithic integration of different types of devices.

We established OMVPE crystal growth techniques as a core technology for the fabrication of semiconductor devices in the late 1980s. We designed the reactor and the gas supply system of OMVPE for realizing ultrafine structure with good uniformity. Excellent uniformity over a 2-inch wafer with monolayer hetero-interface abruptness was obtained ^{(10),(11)}.

3. Device Application

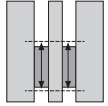
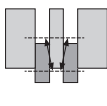
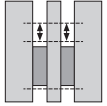
3-1 Semiconductor lasers for communication

The performance of semiconductor lasers has been tremendously improved by applying quantum well structure. Without this technology, a full-fledged commercialization of semiconductor lasers would not be possible. The first operation of a quantum well laser was reported by Van der Ziel et al. ⁽⁵⁾ in 1975. We applied quantum well structure to semiconductor lasers used for optical communication from the late 1980s, and introduced full OMVPE process for mass production. Then high performance lasers, including 1.3 μm Fabry-Perot lasers, 1.48 μm fiber amplifier pumping lasers, and uncooled DFB lasers, have been commercialized ⁽⁹⁾.

Recent explosive increase of traffic in transmission network requires the expansion of transmission capacity of the network. Much effort has been made to increase the capacity of the network by introducing wavelength division multiplexing (WDM) and multi level modulation. With the development of these multiplexing and modulation technologies, intensive study for increasing modulation speed of the device is being performed.

The modulation speed of a semiconductor laser is limited by mainly 2 factors, relaxation oscillation frequency and parasitic impedance. In order to further increase the relaxation oscillation frequency, we introduced compressive strain in the quantum well by lattice mismatch and adopted an AlGaInAs material system whose conduction band offset is larger than that of a conventionally used

Table 1. Summary of application areas of the device and quantum well structure

Wavelength	1	1.5	2	2.5	3	5	8	10 (μm)
	NIR (Near Infrared)					MIR (Mid-infrared)		
Application Field	Information communications Fiber communication		Life sciences Hyperspectrum imaging		Environment/Security Gas sensing, Remote sensing Thermography			
Device	Laser, modulator		Image sensor		Quantum cascade laser			
Quantum Well Structure								
Type	Type I		Type II		Type I			
Transition	Band to band		Adjacent band to band		Inter-subband			
Material	GaInAsP/InP Al(Ga)InAs/InGaAs		InGaAs/GaAsSb		AllnAs/InGaAs			

GaInAsP material system.

It is expected to improve laser gain by introducing compressive stain which induces the reduction of effective hole mass. In addition to the increase of gain, it is also expected to improve temperature characteristics by using the AlGaInAs material system due to the suppression of the carrier leakage at high temperature.

In order to reduce parasitic capacitance, we applied BCB (Benzocyclobutene) for planarization. **Figure 2** shows a schematic illustration of a planar buried BCB ridge-waveguide DFB laser.

Figure 3 shows the dependence of the relaxation oscillation frequency of the device with a cavity length of 250 μm on the bias current at room temperature. Relaxation oscillation frequency extended to about 15 GHz and modulation efficiency (amount of change to the relaxation oscillation frequency of the injected current) of 3.1 GHz/ $\text{mA}^{1/2}$ were obtained at room temperature. Electrical bandwidth was greater than 20 GHz and good eye opening was obtained at 26 Gbit/s, as shown in the figure. These results show that this directly modulated laser is promising for applications in excess of 10 Gbit/s operation. ^{(12), (13)}.

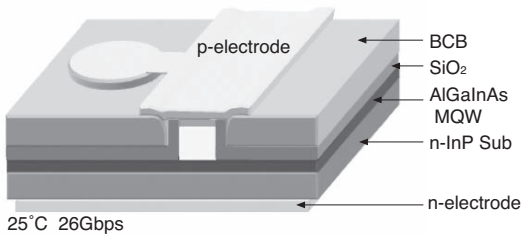


Fig. 2. Planar buried BCB ridge-waveguide DFB laser

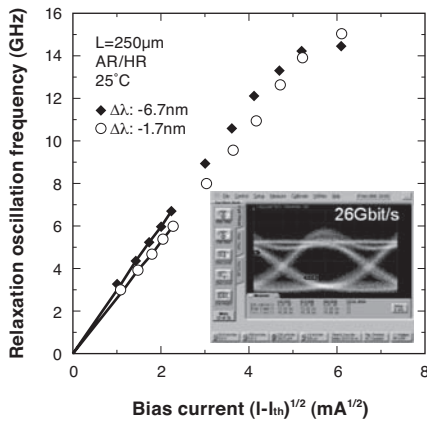


Fig. 3. Bias current dependence of relaxation oscillation

3-2 Electro-absorption modulator integrated with DFB laser

A directly modulated laser (DML) is not suitable for long-distance transmission, since the oscillation wavelength fluctuation (chirp) of DML is relatively large due to the re-

fractive index change by current injection. Therefore, an electro-absorption modulator (EAM) integrated with a DFB laser (EML) has been used for a long-distance transmission light source. The modulation of EML is performed by changing the electric field in quantum well, which changes the absorption edge of the modulator.

The schematic of the operation principle is shown in **Fig. 4**. The quantized energy level formed in the well is changed by the deformation of energy potential induced by the electric field. This is called quantum confined stark effect (QCSE). For type I quantum well structure, this QCSE reduces the effective band gap of the modulator by applying the electric field. So the absorption edge shifts toward longer wavelengths, and then the light is absorbed in the waveguide of the modulator.

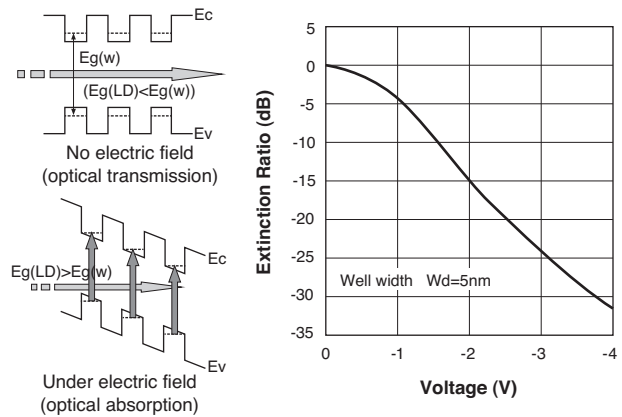


Fig. 4. Principle of EAM and extinction characteristics

Since EML operates without carrier injection, high speed modulation with a low chirp due to a small refractive index change can be realized. Therefore, EML is suitable for high speed mid- and long-distance transmission application.

We fabricated EML by integrating a 1.3 μm DFB laser and EAM consisting of GaInAsP MQW structure with the butt joint using selective growth technique. The butt joint enables each device to be optimized independently with low loss connection. The reduction of parasitic impedance and lateral current confinement structure was made by embedding high mesa waveguide formed by dry etching with

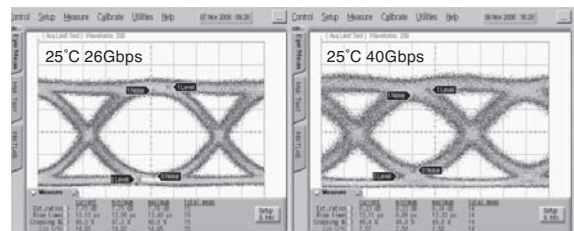


Fig. 5. Eye pattern of EML at 26 and 40 Gbit/s

semi-insulating Fe-InP.

The device operates up to 40 Gbit/s at 25°C with clear eye-opening as shown in Fig. 5. It is expected that EML can be applied not only for 100 Gbit/s but also for 320 Gbit/s (40 Gbit/s x 8 wavelengths) systems in the near future⁽¹⁴⁾.

3-3 Quantum Cascade Laser (Application to environment and security)

In the mid-infrared region (3-10 μm), there are many fundamental vibrations of the molecules. Since these vibrations have 3 to 4 orders of magnitude higher absorption coefficient than those of the harmonics existing in the near-infrared region, high-sensitive gas sensing can be realized. Therefore, many kinds of applications, such as environmental monitoring, semiconductor process control, combustion diagnostics of engines, and medical diagnostics (breath diagnostics), are expected. In addition, the processing of polymeric materials which have large absorption in this spectrum range, and high speed space communication using atmospheric windows are also considered.

In order to realize the mid-infrared semiconductor lasers, it is necessary to match the lattice constant of substrate, cladding layer, and active layer whose band gap corresponds to the oscillation wavelength. There exists several material combinations satisfied this condition such as IV-VI compound semiconductors (PdSnTe). However, it is difficult to realize room temperature operation with reasonable reliability due to the difficulty of crystal growth with high quality and inevitable auger recombination loss. A quantum cascade laser (QCL)⁽⁵⁾ invented in 1994 has solved these problems.

QCL is a laser that can operate in a long wavelength region beyond 3 μm by applying the unique feature of quantum well structure, inter-subband transition and carrier transport by tunneling effects. Figure 6 shows band structure of the QCL. The active region of QCL consists of a multi-tiered unit which is composed of light emitting layers by subband transition and injection layers for carrier transportation by tunneling effects. Optical gain is generated when the carrier flows step-like energy potential like a sequential waterfall (cascade). QCL is a unipolar device which is composed of a single conductive type material, and has fundamentally different principles of operation from the conventional semiconductor laser which is a bipolar device having a p/n junction. In addition, the oscillation

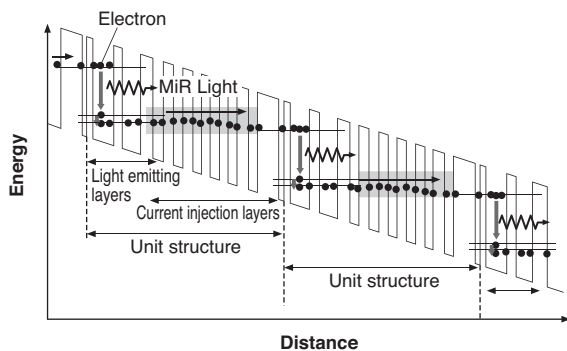


Fig. 6. Band structure of QCL

wavelength of QCL is determined by the quantum well structure, and so far laser oscillation in the range from 3 to 20 μm and the terahertz region has been achieved.

In order to improve the performance of the laser, it is important to improve the probability of inter-subband transitions, as well as to suppress non-radiative transitions. The major non-radiative transition process is longitudinal optical phonon (LO phonon) scattering. To suppress the LO phonon scattering, the active region is designed for a diagonal-transition which occurs between adjacent wells⁽¹⁴⁾. However, in this structure radiative transition probability is small. In contrast, the probability of radiative transitions in vertical transition which occurs in the same well is higher, and at the same time, the probability of LO phonon scattering becomes high. Therefore, if the latter dominates, trade-offs between radiative transition and LO phonon scattering leads to a decrease in laser gain.

We designed a new vertical-transition active layer structure that is expected to increase laser gain by increasing radiative transition probability while suppressing the LO phonon scattering^{(15),(16)}. The active region is formed with AlInAs/GaInAs superlattices, and light emitting layers are composed of three GaInAs quantum wells and two AlInAs barrier layers. The electron injection side of the light emitting layers, which are composed of two GaInAs quantum wells and one AlInAs barrier layer, are designed to enhance vertical transition between the sub-band, so that the probability of radiative transition increases significantly compared to LO phonon scattering. The device was grown by OMVPE on InP substrate. A Fabry-Perot (FP) device has been processed for double channel structure in which current confinement structure is formed by wet etching.

Figure 7 shows temperature dependence of threshold current density of two devices, namely diagonal transition type and vertical transition type, operating at 7 μm region. Stripe width and cavity length of the device are 10 μm and 2 mm, respectively. The device designed for the vertical transition type showed lower threshold current density especially at high temperature. Characteristic temperature, which is a measure of temperature dependence of the threshold current, was 560 K (temperature range 77-150 K) and 127 K (temperature range 150-300 K). This indicates that vertical transition design in the active region is effective to increase radiative transition probability and im-

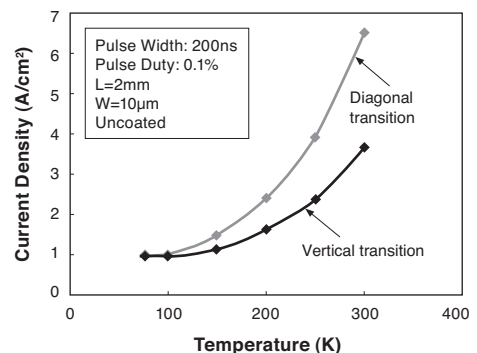


Fig. 7. Temperature dependence of threshold current density

prove the device performance.

The DFB laser was also fabricated in the same manner of the FP laser fabrication. A complex refractive index grating was formed on the contact and upper cladding layer by dry etching and embedding with the upper electrode. **Figure 8 and Fig. 9** show current - optical output characteristics and oscillation spectrum of DFB-QCL (2 mm cavity length, 10 μm mesa width), respectively. Room temperature (300 K) single-mode oscillation with a side mode suppression ratio (SMSR) over 30 dB was obtained and temperature dependence of the oscillation wavelength was 0.4 nm/K. The wavelength tunable operation can be possible by controlling temperature, and QCL is expected to be applied for gas sensing which requires the identification of many sharp absorption spectra existing in the mid-infrared region.

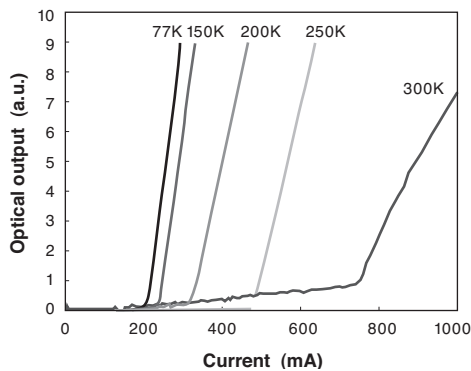


Fig. 8. Current-optical output power characteristics

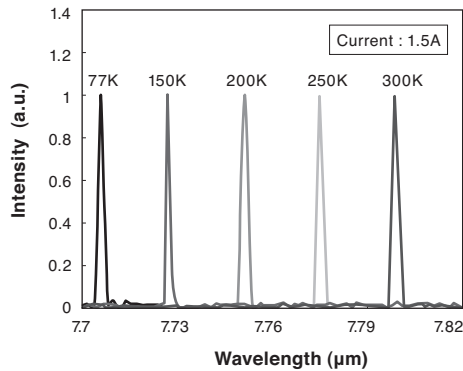


Fig. 9. Oscillation spectrum of QCL

3-4 Near-infrared sensor for life-science application

In this session, the development of the type II quantum well near-infrared imaging sensor which has responsivity up to 2.5 μm is described.

A semiconductor photodetector is a device that transforms light intensity change to current or resistance change by the generation of electrons and holes. Electrons and holes generated by light absorption must be transported quickly without losing through a recombination in

the photodetector. For this reason, there is no advantage to use quantum well structures which have many potential barriers for electrons and holes. Therefore, a bulk material which does not form any hetero-barrier has been used for the photodetector. For example, a bulk InGaAs is employed for the absorption layer of a pin photodetector operating 1.5 μm region. However, in the longer wavelength region beyond 1.5 μm , there is no suitable high quality bulk material for the photodetector. In addition, there is a fundamental problem that the noise current induced by auger recombination and thermal excitation increases with increasing wavelength.

In the wavelength region from 1.5 to 3 μm , there are many harmonics of fundamental vibrations of the molecules. Although their absorption is weak compared with that of fundamental vibrations existing in the mid-infrared region, the light can penetrate deep inside of materials. Therefore, it is suitable for nondestructive measurement of inside of materials. In recent years, there is a growing interest in near-infrared spectroscopy in terms of safety management and quality control in many production sites in industries including the pharmaceutical industry and food industry. It is expected to realize the inspection equipment that can visualize the distribution of concentration and difference in composition by non-destructive, non-invasive measurement at real time. Since the absorption by harmonics of fundamental vibrations is weak, high sensitivity and low noise operation are required for the sensor. However, there is no sensor operating in this wavelength region.

Table 2 shows the comparison of sensor structures grown on InP substrate. The InGaAs lattice matched to the InP substrate shows low dark current and high optical response. However, the spectrum range that can be used for analysis is limited up to 1.7 μm . By increasing In composition of InGaAs, cut-off wavelength can be extended to about 2.6 μm . However, the dark current will increase due to the generation of crystal defects by a large lattice mismatch. In addition, it will be difficult to obtain a highly uniform epitaxial wafer for two dimensional array with a large area. In the present, HgCdTe (MCT) is used for two dimensional array, however, the MCT sensor needs a refrigerator due to a large dark current and it will be expensive.

Table 2. Material comparison for near-infrared sensor

	InGaAs	Extended-InGaAs	InGaAs/GaAsSb
Wavelength	0.9~1.7 μm	0.9~2.6 μm	0.9~3.0 μm
Substrate	InP	InP	InP
Lattice matching	matched	mismatched	matched
Dark current	Low	High	Low
Epitaxial structure			
Remarks	Optical communication PD	InAsP step buffer for lattice mismatch	Type II quantum well structure

Moreover, heavy metals, such as Hg and Cd, give a large impact on environment.

On the other hand, a new materials system, InGaAs/GaAsSb type II quantum well structure, is expected to extend cut-off wavelength up to about 3 μm with lattice-matching to the InP substrate⁽¹⁷⁾⁻⁽¹⁹⁾. The band structure of the type II quantum well is shown in Fig. 10. In this structure, electrons and holes are confined in the InGaAs well and the GaAsSb well respectively, then the transition occurs between InGaAs conduction band and GaAsSb valence band, which corresponds to the wavelength ranging from 2 to 3 μm . Since this material system can be lattice matched to the InP substrate, the generation of crystal defects by lattice mismatch will be eliminated. Therefore, low dark current can be expected. Moreover, a noise current induced by auger recombination and thermal excitation is also expected to be reduced since the type II structure is composed of large band gap materials.

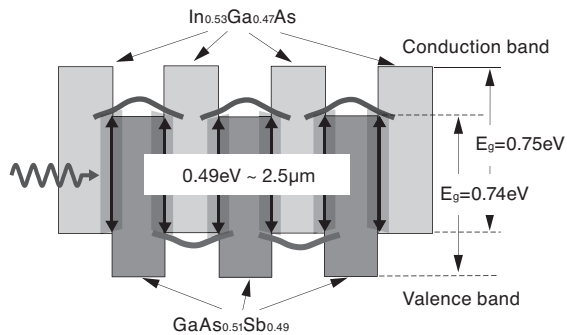


Fig. 10. Band structure of InGaAs/GaAsSb type II quantum well

InGaAs/GaAsSb type II quantum well structure has been grown on InP substrate by OMVPE⁽²⁰⁾⁻⁽²³⁾. The structural characterization was done by X-ray diffraction. Figure 11 shows X-ray diffraction pattern of the type II quantum well structure (layer thickness 5 nm/5 nm, number of quantum well pair 50). Sharp satellite peaks, which were in good agreement with simulated diffraction patterns, indicate good structural quality of the epitaxial layer.

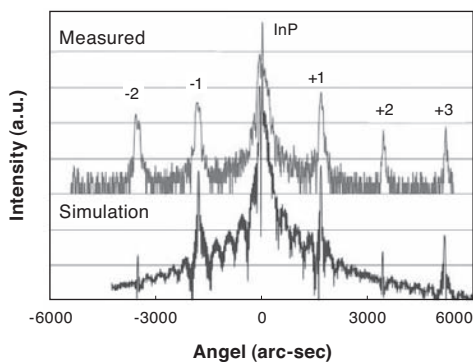


Fig. 11. X-ray diffraction pattern of InGaAs/GaAsSb type II quantum structure

Photoluminescence (PL) measurement was also carried out for optical characterization of the type II quantum well structure. Figure 12 shows PL spectrum of the quantum well at room temperature. Clear photoluminescence with peak wavelength of 2.43 μm corresponding to type II transition was observed.

We fabricated a pin photodetector whose absorption layers consist of type II quantum well structure as shown in Fig. 13. A Si-doped InGaAs buffer layer, InGaAs/GaAsSb quantum well absorption layers (thickness of each layer 5 nm/5 nm, number of quantum well pair 250), undoped InGaAs layer, and Si-doped InP layer were grown by OMVPE. Then, a p/n junction was formed by selective Zn diffusion using SiN mask. SiON film was used as an anti-reflection coating, and finally, p and n electrodes were formed with AuZn and AuGeNi, respectively.

Dark current of a 15 $\mu\text{m}\phi$ device was 5.3 pA with reversed bias of 60 mV at -40°C , which corresponds to a dark current density of 3 $\mu\text{A}/\text{cm}^2$. This dark current, which was proportional to the photo detection area, was attributed to the recombination generation current in the absorption region.

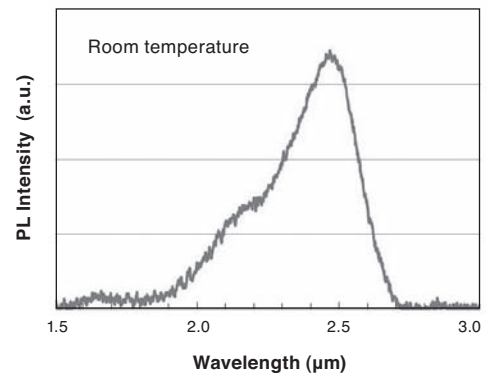


Fig. 12. Photoluminescence spectrum of InGaAs/GaAsSb type II quantum structure

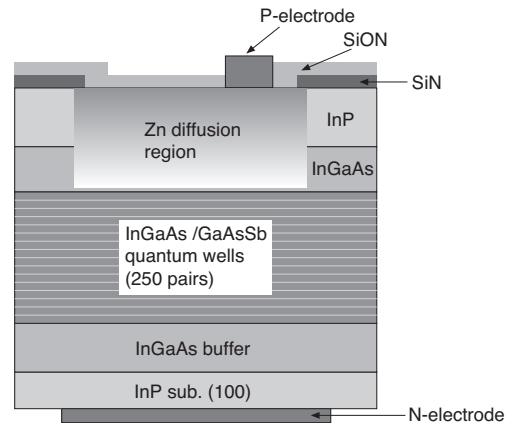


Fig. 13. Cross-sectional view of detector

Figure 14 shows temperature dependence of dark current of InGaAs/GaAsSb quantum well and an HgCdTe detector with the photo detection diameter of 15 μm . The dark current of the InGaAs/GaAsSb quantum well detector was about one order of magnitude smaller than that of the HgCdTe detector at the same temperature. This clearly indicates that InGaAs/GaAsSb quantum well structure has a high potential for low noise detector application. **Figure 15** shows responsivity of the photodetector. Photoresponse extended to about 2.5 μm corresponds to the type II quantum well absorption edge.

A two-dimensional imaging sensor integrating 320 x 256 photodetectors mentioned above was fabricated. The photo detection diameter of each device is 15 μm and pixel size is 30 x 30 μm . The sensor chip was bonded to read out IC (ROIC) with indium micro-bump, and assembled in a ceramic package with peltier device (**Photo 1**). High linearity and low noise characteristics with small variation of dark current ranging from 4 to 8 pA at -40°C were obtained. This sensor was built in the camera, and a near-infrared imaging system using this camera has been commercialized under the trade name "Compovision" ⁽²⁴⁾.

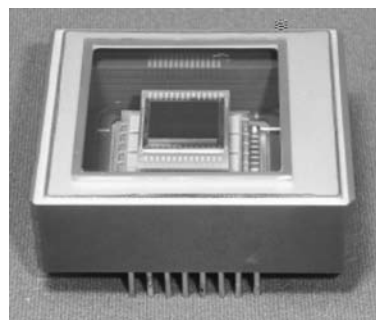


Photo 1. Near-infrared imaging sensor

4. Conclusion

Semiconductor quantum well structure, including superlattice structure, is a new material based on the concept of quantum mechanics, one of the greatest inventions in the 20th century. It shows unique properties that cannot be obtained in bulk materials. These properties of the quantum well structure have enabled opto-electronic devices to have various new functions and high performance.

In this paper, we described a variety of optical devices composed of quantum well structures, including semiconductor laser and modulator for high speed application in optical communication, quantum cascade laser for high sensitive gas detection, and near-infrared imaging low noise sensor for various applications in life sciences. These devices show superior performance and new features that cannot be realized in conventional devices. Quantum well technology will continue to be a driving force in the development of compound semiconductor devices. Attractiveness of this technology is endless.

* Compovision is a trademark or registered trademark of Sumitomo Electric Industries, Ltd.

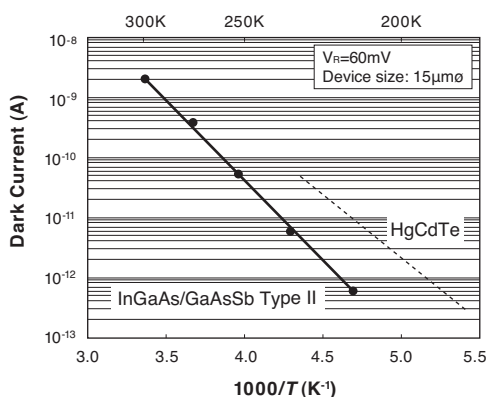


Fig. 14. Temperature dependence of dark current InGaAs/GaAsSb and HgCdTe photodetector

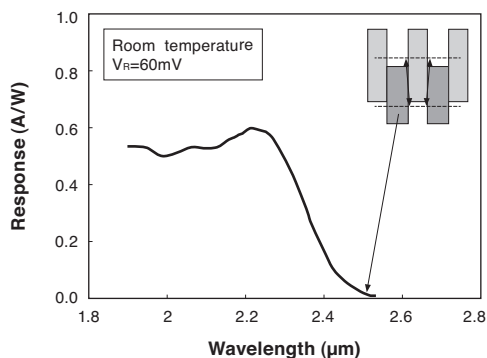


Fig. 15. Responsivity of InGaAs/GaAsSb quantum well photodetector

References

- (1) L. Esaki et al. "Superlattice and negative differential conductivity in semiconductors," IBM Journal of Research and Development, vol. 14 No1 p61 (1970)
- (2) R. Dingle et al. "Electron Mobilities in Modulation-Doped Semiconductor Heterojunction Superlattices," Appl. Phys. Lett. 33 p665 (1987)
- (3) T. Mimura et al. "A New Field-Effect Transistor with Selectively Doped GaAs/n-Alx Ga1-x As Heterojunctions," Jpn. J. Appl. Phys. 19, L225 (1980)
- (4) L. L. Chang et al. "Resonant tunneling in semiconductor double barriers," Appl. Phys. Lett. 24, p593, (1974)
- (5) J. P. van der Ziel, et al., "Laser oscillation from quantum states in very thin GaAs-Al0.2Ga0.8As multilayer structures," Appl. Phys. Lett. 26, 463 (1975)
- (6) Y. Arakawa et al. "Multidimensional quantum well laser and temperature dependence of its threshold current," Appl. Phys. Lett. 40 (11), p939 (1982)

- (7) J. Faist, et al. "Quantum Cascade Laser," Science Vol.264, 22, p553 (1994)
- (8) H. Hayashi, "Development of Compound Semiconductor Devices - In Search of Immense Possibilities -," SEI Technical Review, No72, p4 (2011)
- (9) T. Katsuyama, "Development of Semiconductor Laser for Optical Communication," SEI Technical Review, No69, p13 (2009)
- (10) H. Kamei et al., "OMVPE growth of GaInAs/InP and GaInAs/GaInAsP quantum well," J. Crystal Growth, p567 (1991)
- (11) T. Katsuyama et al., "Highly uniform GaInP and AlGaInP/GaInP QW structures grown by organometallic vapor phase epitaxy," Pro. of the 16th GaAs Related, Institute of Physics Conference Series, No 106, p.12 (1989)
- (12) H. Yagi et al., "26 Gbit/s Direct Modulation of AlGaInAs/InP Lasers with Ridge-Waveguide Structure Buried by Benzocyclobutene Polymer," IPRM (2009)
- (13) K. Tawa et al., "Study on the 1.3 μ m LAN-WDM transmission system using 40Gbps EML," Proc. The Institute of Electronics, Information and Communication Engineer General Conference B-8-34 (2009)
- (14) J. Faist, et al. "Quantum Cascade Laser: Temperature dependence of the performance characteristics and high T₀ operation," Appl. Phys. Lett., 65, p2901 (1994)
- (15) J. Hashimoto et al., "Mid-IR(7~8 μ m) Vertical transition quantum cascade laser," The Japan Society of Applied Physics Conference, 28a-p8-5.(2011)
- (16) J. Hashimoto et al., "Mid-IR vertical transition DFB quantum cascade laser," The Institute of Electronics, Information and Communication Engineer Society Conference (2011)
- (17) G. A. Sai-Halasz et al., "A new semiconductor superlattices," Appl. Phys. Lett., Vol 30, p651 (1977)
- (18) A. Yamamoto et al., "Optical properties of GaAs_{0.5}Sb_{0.5} and In_{0.53}Ga_{0.47}As/GaAs_{0.5}Sb_{0.5} type II single hetero-structures lattice-matched to InP substrates grown by molecular beam epitaxy," J. Cryst. Growth 201, p872 (1999)
- (19) R. Sidhu et al., "A long-wavelength photodiode on InP using lattice-matched GaInAs-GaAsSb type-II quantum wells," IEEE Photon. Technol. Lett. 17, p2715 (2005)
- (20) H. Inada et al., "Low Dark Current SWIR Photodiode with InGaAs/GaAsSb Type II Quantum Wells Grown on InP Substrate," SEI Technical Review, No70, p100 (2010)
- (21) Y. Iguchi, "Development of InGaAs/GaAsSb typeII quantum well infrared sensor," The Japan Society of Applied Physics (2011)
- (22) H. Inada et al., "MOVPE grown InGaAs/GaAsSb Type II Quantum Well Photodiode for SWIR Focal Plane Array," SPIE DSS (2011)
- (23) H. Inada et al. "Uncooled SWIR InGaAs/GaAsSb type II quantum wells focal plane array," SPIE DSS (2010)
- (24) Y. Kobayashi et al., "Real time composition imaging system 'Composition'," Optonews (in Japanese) p63 Vol.5, No.2 (2011)

~~~~~

**Contributors** (The lead author is indicated by an asterisk (\*).)

**T. KATSUYAMA**

- Senior Specialist  
 Doctor of Engineering  
 Manager, Transmission Device R&D Laboratories

